Bioorganic & Medicinal Chemistry 18 (2010) 1516–1525

Contents lists available at ScienceDirect

Bioorganic & Medicinal Chemistry

journal homepage: www.elsevier.com/locate/bmc

# Novel matrix metalloproteinase inhibitors derived from quinoxalinone scaffold (Part I)

Yonggang Li, Jian Zhang, Wenfang Xu, Huawei Zhu, Xun Li *

*School of Pharmaceutical Sciences, Shandong University, No. 44 WenhuaXi Road, Ji'nan, 250012 Shandong Province, PR China*

ARTICLE INFO

*Article history:*
Received 27 November 2009
Revised 31 December 2009
Accepted 5 January 2010
Available online 11 January 2010

*Keywords:*
Quinoxalinone derivatives
MMP-2 inhibitors
Peptidomimetic
Anti-tumor

ABSTRACT

A series of quinoxalinone peptidomimetic derivatives was designed, synthesized, and assayed for their inhibitory activities on metalloproteinase-2 (MMP-2) and aminopeptidase N (APN). The results showed that all of these quinoxalinone derivatives displayed highly selective inhibition against MMP-2 as compared with APN, with $IC_{50}$ values in the micromole range. Compound **A3** showed comparable MMP-2 inhibitory activities than the positive control LY52, which might be used as a potential lead in future research on anticancer agents.



## 1. Introduction

Matrix metalloproteinases (MMPs) are a family of structurally and functionally related zinc-dependent endopeptidases that are involved in the degradation of the extracellular matrix (ECM) proteins as well as the tumorgenesis process and, consequently, they play a crucial role in physiological processes such as tissue remodeling, apoptosis and wound healing. As the overregulation of MMPs is involved in many inflammatory, malignant and degenerative conditions, attempts to design and exploit inhibitors that may modulate their regulation have become of great interest.[1–3]

Up to date, many reported broad-spectrum inhibitors exhibit a poor selectivity as a consequence of the high structural similarity among the members of the MMP family. Even if the low specificity does not prevent the use in vivo, it raises a variety of side effects and it also limits the dose that may be daily administered. As a result, clinical trials conducted on these broad-spectrum inhibitors have yielded disappointing results, especially in the cancer pathology area. Accordingly, the search of appropriate MMP inhibitor (MMPI) with high potency and selectivity for certain subtypes still represents an important pharmaceutical target.[4] Among the identified more than 20 structurally related family members, MMP-2 (gelatinase A) is highly involved in the process of tumor invasion and metastasis, which has been a promising target for cancer therapy.[5,6]

It has been reported that besides the catalytic activity center zinc ion of MMP-2, there are two hydrophobic domains, which are called $S_1'$ and $S_2'$ pocket, respectively. $S_1'$ pocket, the key domain to characterize the selectivity of various MMPs, is deeper and narrower than that of most other MMP subtypes, while $S_2'$ pocket is solvent exposed.[7,8] Currently identified MMP-2 inhibitors have several structural characteristics and binding mode: (1) a zinc-binding group (ZBG) capable of chelating with the zinc ions and sequentially inhibiting the metastatic spread of tumors;[9] (2) at least one functional group, which provides at least a hydrogen bond interaction with the enzyme backbone; and (3) one or more lipophilic residues that can be accommodated in at least one of the subsites of the enzyme active sites, such as $S_1'$ and $S_2'$ pockets.[10]

Enlightened by these findings, our group has previously reported a series of novel MMP-2 inhibitors with remarkable MMP-2 inhibitory activities in the enzymatic assays.[11–16] One of the inhibitors, LY52 (see Fig. 1), a caffeinoyl pyrrolidine derivative, manifested satisfactory potency against MMP-2 with $IC_{50}$ value in the nanomolar range. This compound could significantly suppress the invasion and metastasis of human carcinoma cells via inhibition of MMP-2 proteolytic activities.[17,18] LY52 was thereby used as a positive control to elucidate the enzymatic activities.

In our continuous program in the search of new potent MMP-2 inhibitors, a new class of molecular heterocyclic scaffold, quinoxalinone (or quinoxalin-2-one), an important pharmacophore in numerous bioactive compounds, was chosen to design selective MMP-2 inhibitors.[19] The main features of this scaffold include: (1) the electron donor and/or acceptor of the quinoxalinone core might generate effective interactions with the enzyme backbone, (2) the quinoxalinone moiety can be decorated with a ZBG and a lipophilic residue to insert into the hydrophobic $S_1$ pocket, (3) the synthesis comprises only few steps starting from commercially

* Corresponding author. Tel./fax: +86 531 88382264.
*E-mail address:* tjulx2004@sdu.edu.cn (X. Li).

0968-0896/$ - see front matter © 2010 Elsevier Ltd. All rights reserved.
doi:10.1016/j.bmc.2010.01.008

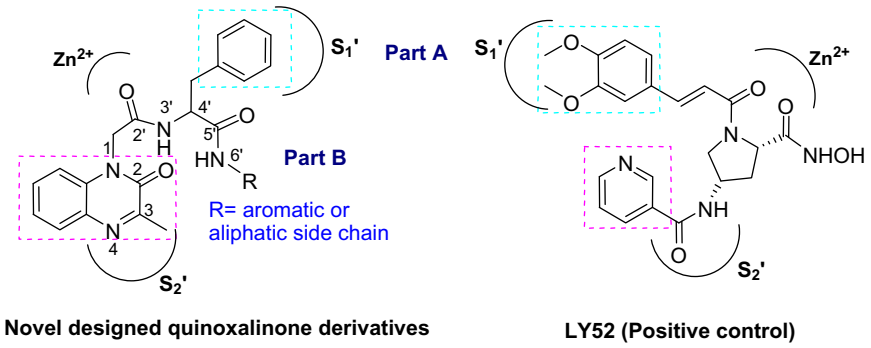


**Figure 1.** The design concept of new quinoxalinone peptidomimetics.

available enantiopure precursors and further stereochemistry control can be easily accomplished and, (4) the quinoxalinone core has a number of positions which can be chemically functionalized leading to molecular diversity. All these properties, together with fair molecular weight, were considered in scaffold selection.

Further optimization on the quinoxalinone scaffold was carried out as follows (Fig. 1): (i) Given many phenylalanine derivatives have been reported to demonstrate significant antitumor activity,[20,21] L-phenylalanine moiety was, therefore, introduced to mimic the caffeinoyl fragment of LY52 (Part A), and construct the first integrated peptidomimetic pattern (O=C2′–N3′H) to interact with the $S_1'$ pocket of MMP-2; (ii) Incorporating a range of aromatic or aliphatic primary amines to connect with the 5'-carboxyl group of phenylalanine so as to build another peptidomimetic pattern (Part B), and the carbonyl group (C2'=O) served as the zinc-binding group.

In the present study, we hereby describe the synthesis and evaluation of the enzymatic activities of the corresponding quinoxalinone peptidomimetic derivatives, as well as the docking studies of the interaction, with the anticipation of gaining a more efficacious tool compound for tumor therapeutic screening.

## 2. Chemistry

The target compounds were synthesized efficiently following the procedures outlined in Scheme 1. Meanwhile, the chemical structures of the target compounds were analytical confirmed by IR, $^1$H NMR, and ESI-MS (see Section 5).

In our synthesis, the quinoxalinone scaffold **1** was easily prepared from the commercially available *o*-phenylenediamine following the reference.[22] Subsequent nucleophilic substitution was accomplished using ethyl 2-oxopropanoate in the presence of anhydrous ethanol, followed by hydrolization of ester group to the carboxylic acid **3**, which was condensed with L-phenylalanine methyl ester to provide compound **4**. This compound was further hydrolyzed to offer the carboxylic compound **5**, and the key intermediate acyl chloride **6** was then obtained via the acylation. This was followed by coupling with various aromatic or aliphatic primary amines in the existence of *t*-BuOK in anhydrous $CH_2Cl_2$ to provide the target compounds **7**. In this reaction, apart from $CH_2Cl_2$, other aprotic polar solvents such as benzene can also be preferable.

## 3. Results and discussion

### 3.1. Structure–activity relationship (SARs) studies

The target quinoxalinone peptidomimetic derivatives were evaluated for their enzymatic inhibition on MMP-2 and APN/CD13, and the results are listed in Table 1. Similar to MMP-2, APN is also a zinc-dependent metalloproteinase involved in the process of tumor invasion and metastasis.[23,24] Hence the assay

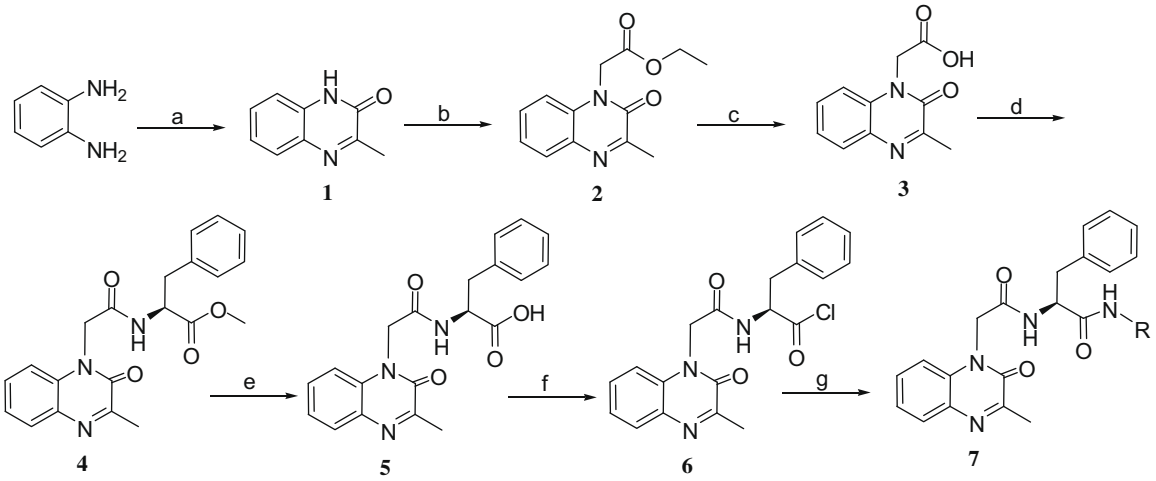


**Scheme 1.** Reagents and conditions: (a) ethyl 2-oxopropanoate, anhydrous EtOH; (b) Ethyl chloroacetate, $K_2CO_3$, reflux; (c) KOH solution, EtOH, then concentrated HCl; (d) L-phenylalanine methyl esters, HOBT/EDCI/$Et_3N$, anhydrous $CH_2Cl_2$; (e) KOH, EtOH, then concentrated HCl; (f) sulfuryl dichloride, anhydrous $CH_2Cl_2$; (g) *t*-BuOK, anhydrous $CH_2Cl_2$, rt.

**Table 1**
In vitro enzymatic assay (MMP-2 and APN) results for target compounds

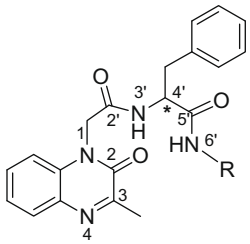

| Compds | R | $IC_{50}$ (μM)[a] | |
|---|---|---|---|
| | | MMP-2 | APN/CD13 |
| **A1** | 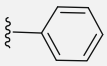 | 58.14 ± 3.0* | NA[b] |
| **A2** | 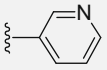 | 30.05 ± 1.6* | NA[b] |
| **A3** | 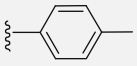 | 10.49 ± 2.4** | NA[b] |
| **A4** | 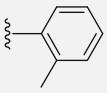 | 37.29 ± 5.7** | NA[b] |
| **A5** | 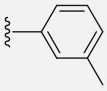 | 6460.8 ± 1.3 | NA[b] |
| **A6** | 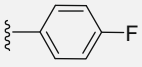 | 124.32 ± 2.4 | NA[b] |
| **A7** | 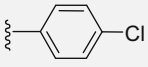 | 624.48 ± 1.1 | NA[b] |
| **A8** | 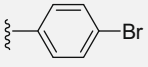 | 2000 ± 7.3 | NA[b] |
| **A9** | 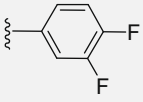 | 24.18 ± 6.6** | NA[b] |
| **A10** | 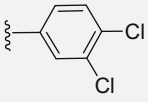 | 26.17 ± 1.6* | NA[b] |
| **A11** | 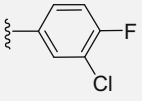 | 1362.8 ± 2.4 | NA[b] |
| **A12** | 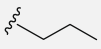 | 56.6 ± 4.5** | NA[b] |
| **A13** | 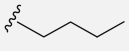 | 106 ± 1.2 | NA[b] |
| **A14** |  | 105.3 ± 7.8 | NA[b] |
| **A15** |  | 9426.5 ± 3.6 | NA[b] |
| **A16** | 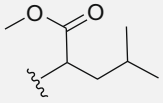 | 1750 ± 2.6 | NA[b] |
| **A17** | 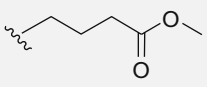 | 2757.8 ± 1.8 | NA[b] |

**Table 1** (*continued*)

| Compds | R | $IC_{50}$ (μM)[a] | |
|---|---|---|---|
| | | MMP-2 | APN/CD13 |
| **A18** | 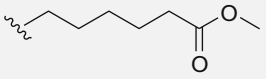 | 11520 ± 3.3 | NA[b] |
| **A19** | 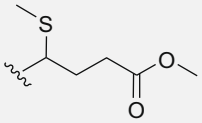 | 1920.5 ± 0.9 | NA[b] |
| LY52 | 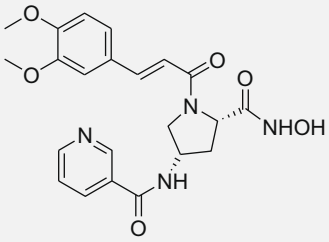 | 5.6 ± 0.6 | NA[b] |

[a] Values are means ± standard error of three experiments. * $p$ <0.01, ** $p$ <0.05 compared to the control (LY52).
[b] Not activity.

was performed on both of MMP-2 and APN so as to identify the selectivity of target compounds. And else, LY52 was used as the positive control.

The enzyme inhibitory results unveiled that all of the tested quinoxalinone peptidomimetic derivatives (**A1–A19**) displayed high selectivity against MMP-2 as compared with APN, thus, to a certain extent, validating our strategy for designing MMP-2 inhibitors. This possibly descript from the differences between the structures of two enzymes, leading to different requirements for their respective inhibitors. MMP-2 is a zinc-dependent endopeptidase that could cut the peptide to parts from the specific amino acid residue of the peptide, while APN is a membrane-bound zinc exopeptidase that catalyzed the removal of $NH_2$-terminal amino acid from the peptide.[1,6] As the above mentioned selectivity against APN, the following SARs were mainly discussed about MMP-2 inhibition.

Among these inhibitors, the R groups can be altered from aromatic to aliphatic. Generally speaking, compounds with aromatic side chains (**A1–11**) were found to be more potent than those aliphatic derivatives (**A12–19**). The possible reason might be due to the π system of the aromatic ring enhancing the binding interaction with the hydrophobic region of the enzyme.

The activity of **A2** was better than **A1**, which confirmed that pyridinyl ring is better than phenyl group. This result might be owing to the contribution of electronegative nitrogen atom, which can more easily form hydrogen bond with the enzyme backbone, thus stabilizing the binding between the compound and the enzyme.

Substitution on aromatic ring (**A3–11**) also has impact on bioactivity. For instance, comparing compounds with mono-substitution of methyl group at different positions in the aromatic ring (**A3–5**), methyl-substitution at the *para*-position (**A3**, $IC_{50}$ = 10.49 ± 2.4 μM) displayed the highest affinity, methyl-substitution at the *ortho*-position (**A4**, $IC_{50}$ = 37.29 ± 5.7 μM) was in the next place, while the *meta*-one (**A5**) presented the least activity. Additionally, comparing compounds with halogen-substitution at the *para*-position in the aromatic ring (**A6–8**), it seems that the increased bulk of halogen substituents leads to impaired activity, suggesting there is a space requirement in the binding pockets to accommodate the suitable substituents.

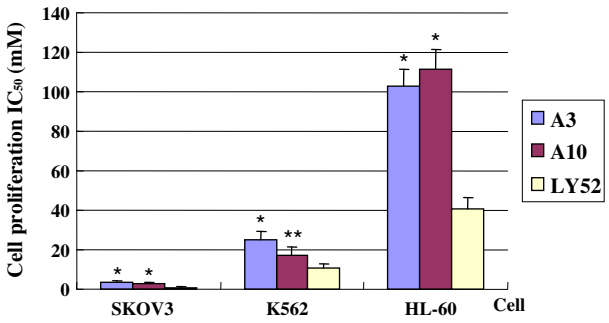


**Figure 2.** Effects of LY52 and compounds **A3** and **A10** on proliferation of the SKOV3, K562 and HL-60 cell lines. Data are expressed as mean values of five independent experiments (±SE). * $p$ <0.01, ** $p$ <0.05 compared to the control (LY52).

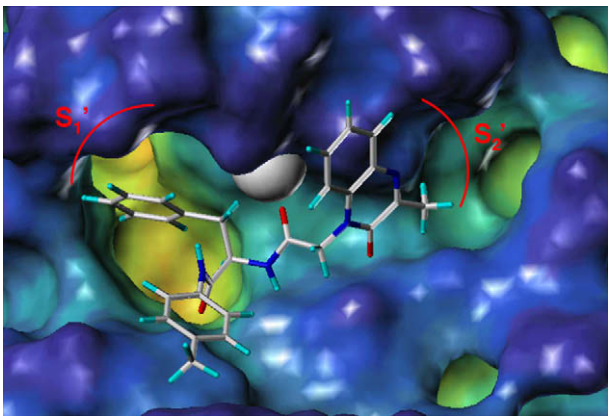


**Figure 4.** FlexX docking result of compound **A3** with MMP-2.

As compared with the halogen-substituted compounds, di-substitution of fluorine or chlorine at the 3-, 4-position of the aromatic moiety (**A9** and **A10**) manifested improved potencies in comparison with the mono-substitution counterparts (**A6** and **A7**). However, when the same position of the phenyl moiety was replaced with fluorine and chlorine (**A11**), severely impaired affinity was observed.

As to the compounds with aliphatic substituents (**A12–19**), the length of the side chain will partly influence the activities of the compounds. Specifically, to some extent, length of R groups was negatively relative with the MMP-2 inhibition, suggesting it is unfavorable to increase the length of substituents along the orientation of the R groups. This might be due to the longer group was unfavorable to the accommodation with the enzymes' hydrophobic domains.

Compound **A16** was found to be more potent than **A15**. This activity difference was probably caused by the carboxylate ($COOCH_3$). As a ZBG and potential prodrug, the carboxylate and its corresponding metabolite carboxylic acid (COOH) can chelate with zinc at the catalytic center of the enzyme, resulting in significantly enzymatic inhibition. Furthermore, as compared with the activities of **A17** and **A19**, the introduction of methylthio ($SCH_3$) produced enhanced potency, suggesting that methylthio group was positively related with the inhibitory activity by forming effective hydrogen bond with the residue of the enzyme.

Finally, the effects of **A3** and **A10** on the proliferation of three tumor cell lines (SKOV3, K562 and HL-60), compared with LY52, were further assessed by using MTT assay, which are shown in Figure 2. In our assay, tumor cell lines were selected according to their expression of MMP-2 and APN, and, the concentrations inducing a 50% inhibition of cell growth ($IC_{50}$) in mM are reported. Among these three cell lines, HL-60 (myelo-monocytic human acute granulocytic leukemia cells having high basal APN activity)[25] and K562 cells (human chronic myelogenous leukemic cells expressing low levels of APN)[26] were selected to verify the APN inhibitory activities of target compounds, while SKOV3 cells (human ovarian carcinoma cells expressing high levels of MMP-2)[27] was selected to investigate the MMP-2 inhibitory activity. The results indicated that the anti-proliferative effects of these two compounds (**A3** and **A10**) against HL-60 and K562 cells (data were not given) were significantly lower than the positive control. This result is consistent with the results of enzyme inhibition. As to the SKOV3 cells, although these two compounds exhibited improved inhibitory effects on cell proliferation with $IC_{50}$ values of 1.98 ± 0.08 mM and 3.02 ± 0.12 mM, respectively, they still gave less potency than LY52 (0.21 ± 0.09 mM).

From the above SAR studies, it can be concluded that although some compounds, for example, **A3**, **A9**, **A10**, gave comparable MMP-2 inhibitory activities with LY52, all of the tested compounds displayed weaker potency in comparison with the positive control. Thereby, further structural optimization should be attentively investigated towards the reported compounds.

### 3.2. Binding mode

Compounds **A3** and **A10** were selected to study their binding mode with MMP-2. Firstly, their predicted conformations were optimized with the Powell Energetic Gradient method built in the Sketch/Build Edit model (SYBYL6.91, Linux 7.3).[28] As compared with the positive control LY52, the comparable results demonstrated the affinity to the same spatial regions ($S_1'$ and $S_2'$), implying the similar MMP-2 inhibitory activities. In precise words, both the caffeinoyl portion of LY52 and the phenyl group of target compounds can adjust their flexibility to extend into the $S_1'$ pocket with their preponderant conformations, as diagrammed in Figure 3. In contrast, the similar situation can be seen between the quinoxalinone fragments of **A3** and **A10** and the pyridinyl-substituted amide portion of LY52.

To further understand the inhibitory difference between the MMP-2 and APN, the preferred pharmacophore docking studies were carried out via the FlexX flexible-Dock program. The interactions of **A3** and **A10** with the active sites of MMP-2 (PDB ID: 1HOV)[29] and APN (PDB ID: 2DQM) were compared, which are shown in Figures 4–7. Not surprisingly, both the two compounds

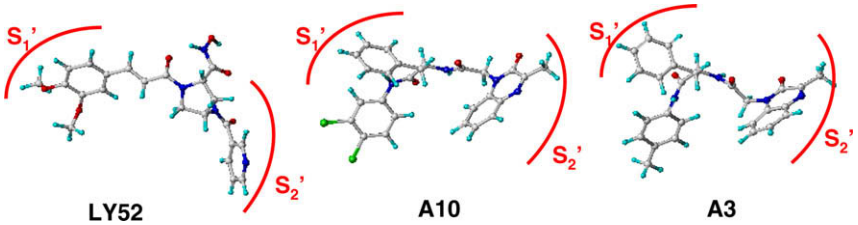


**Figure 3.** Comparison of preponderant conformations between compounds LY52, **A10** and **A3**.

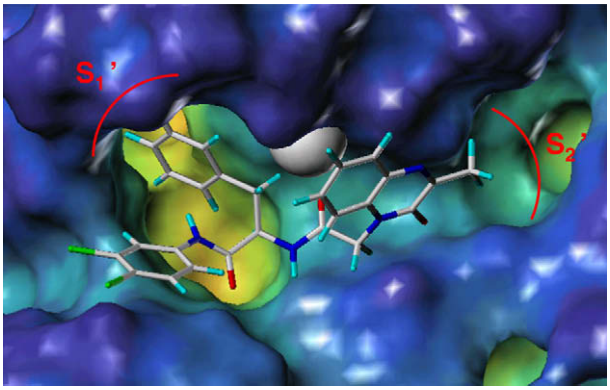


**Figure 5.** FlexX docking result of compound **A10** with MMP-2.

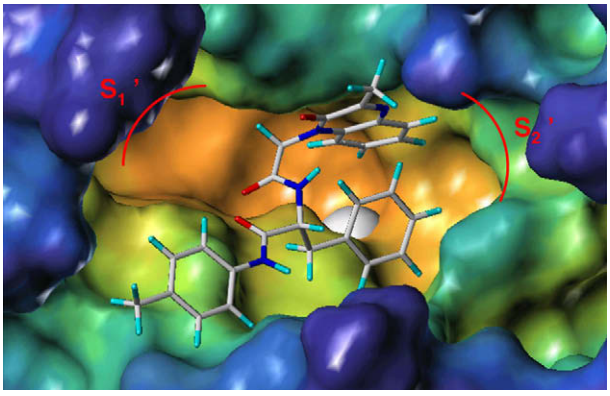


**Figure 6.** FlexX docking result of compound **A3** with APN.

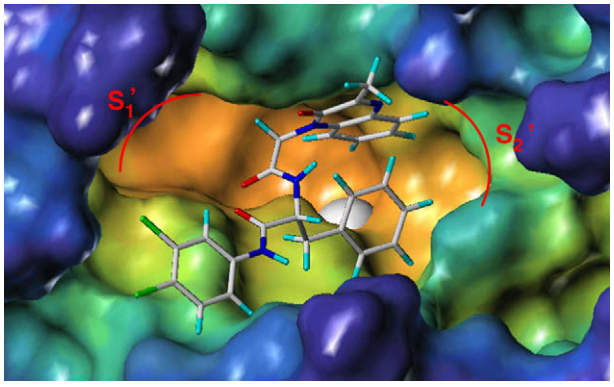


**Figure 7.** FlexX docking result of compound **A10** with APN.

could not well-orienting occupy the active domain ($S_1'$ and $S_2'$ pockets) of APN, resulting in sharply impaired APN inhibition (even has no APN inhibition), consistent with the enzymatic assay results. Unlike the binding situations with APN, the moderate bulk of the quinoxalinone fragments as well as the phenyl groups of the two compounds could undergo torsional motion to allow their suitable conformations to accommodate the $S_1'$ and $S_2'$ pockets, respectively. Besides, the oxygen atom of carbonyl group (O=C2') coordinate with the catalytic zinc ion 166.

Finally, to obtain further insight into the interaction of **A10** with MMP-2, a 2-D picture was also created with the program LIGPLOT. As graphically shown in Figure 8, we can see the backbone of **A10** could form hydrophobic contacts with His85 and Ala86 of $S_1'$ pocket and form hydrogen bond with Ala86 (<2.74 Å) by the carbonyl of quinoxalinone group. The oxygen atom (O15) of carbonyl group coordinated with the zinc ion of MMP-2 with a distance of 1.90 Å. As far as the His120 residue is concerned, the imidazolyl of it can interact with the carbonyl group of **A10** by hydrogen interaction (<3.35 Å) which might be benefit to stabilize of interaction intermediate with the zinc ion. In addition, the binding interactions were further enhanced by hydrogen bonds with Leu83 (<2.89 Å). Besides, the hydrophobic parts of aromatic rings are in contact with nonpolar surface areas of MMP-2.

It should be indicated that although the computed information assay totally supported our assumption, the exact binding model of the target compounds with MMP-2 should be validated from further X-ray crystal studies.

## 4. Conclusions

In summary, we have developed a new series of quinoxalinone peptidomimetic derivatives as potential MMP-2 inhibitors. It should be noted that although all of these compounds display less activity than that of LY52, they possess significant selectivity against MMP-2 as compared with APN. This feature may provide us a critical point for further chemical modification on these quinoxalinone derivatives so as to exploit more potent MMP-2 inhibitors.

## 5. Experimental

### 5.1. General procedures

Unless specified otherwise, all the starting materials, reagents and solvents were commercially available. All reactions except those in aqueous media were carried out by standard techniques for the exclusion of moisture. All reactions were monitored by thin-layer chromatography on 0.25-mm silica gel plates ($60GF_{254}$) and visualized with UV light (254 nm), or iodine vapor. Melting points were determined using X-6 digital display binocular microscope (uncorrected). $^1$H NMR spectra were determined on a *Brucker Avance DRX-600* spectrometer using TMS as an internal standard, $\delta$ in parts per million and $J$ in hertz (Hz). Infrared spectra were measured on a nicolet nexus *470 FT-IR* spectrometer using KBr plate. Electrospray ionization mass spectrometry (ESI-MS) was performed on an *API-4000* triple-stage quadrupole instrument. Measurements were made in $D_2O$ or $CD_3OD$ solutions. Elemental analyses were carried out on a Perkin–Elmer C, H, N elemental analyzer.

### 5.2. Syntheses

#### 5.2.1. 3-Methylquinoxalin-2(1*H*)-one (1)

1,2-Phenylenediamine (10.81 g, 0.10 mol) and ethyl pyruvate (12.77 g, 0.11 mol) were dissolved in 250 ml of anhydrous EtOH and the mixture was stirred for 24 h at room temperature. The crude product spontaneously precipitated in the progress which was collected and recrystallized from anhydrous EtOH to give compound **1** (14.85 g, 92.7%) as yellow needles. Mp 241–243 °C; ESI-MS: 161.0 $[M+H]^+$.

#### 5.2.2. Ethyl 2-(3-methyl-2-oxoquinoxalin-1(2*H*)-yl)acetate (2)

A mixture of compound **1** (8.01 g, 0.05 mol), ethyl chloroacetate (7.353 g, 0.06 mol), anhydrous potassium carbonate (8.29 g, 0.06 mol) and tetrabutyl ammonium bromide (1.61 g, 0.005 mol) was dissolved in 200 ml of acetone, the mixture was successively refluxed for 6 h. The obtained product was crystallized from etha-

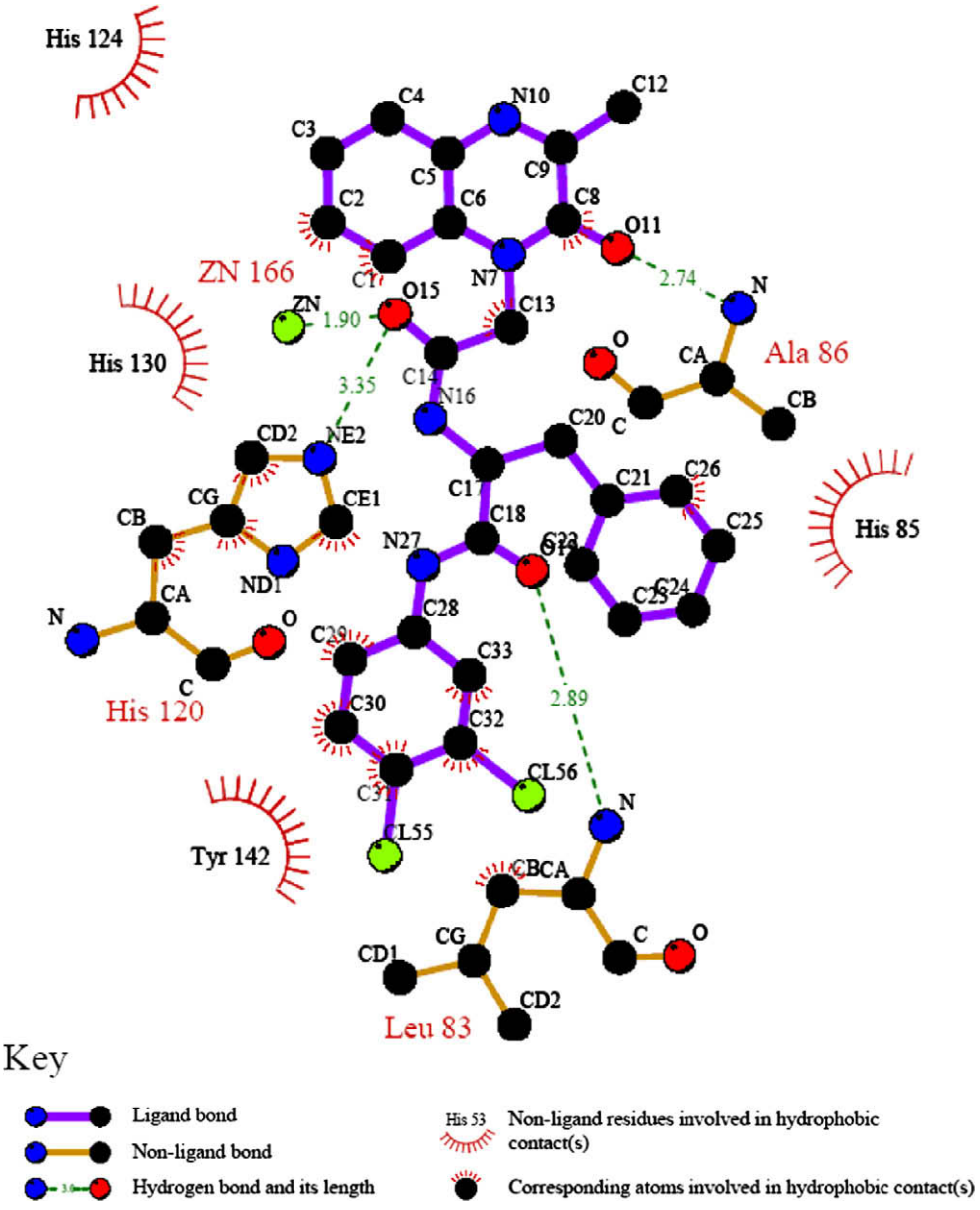


**Figure 8.** The docking result of **A10** with MMP-2 shown by LIGPLOT. Compound **A10** is diagrammed in violet.

nol to give compound **2** as yellow powder (9.013 g, 73.2%). Mp 120–122 °C; $^1$H NMR ($CDCl_3$-$d_6$, ppm): $\delta$ 1.18 (3H, s), 2.62 (3H, s), 4.01 (2H, q), 5.05 (2H, s), 7.05–7.86 (4H, m), ESI-MS: 247.1 $[M+H]^+$.

### 5.2.3. 2-(3-Methyl-2-oxoquinoxalin-1(2*H*)-yl)acetic acid (3)

Compound **2** (4.93 g, 0.02 mol) was suspended in a solution of 1 M KOH/EtOH (80 ml), the suspension was then stirred at room temperature for 6 h. Subsequently, the mixture was allowed to concentrate in vacuo until the pale solid appeared which was acidified to pH 4.0. The obtained precipitated product was collected and crystallized from THF to give compound **3** (3.81 g, 87.3%) as yellow solid. Mp 225–227 °C, ESI-MS: 218.1 $[M+H]^+$.

### 5.2.4. (*R*)-Methyl2-(2-(3-methyl-2-oxoquinoxalin-1(2*H*)-yl)acetamido)-3-phenylpropanoate (4)

Compound **3** (10.91 g, 0.05 mol) and HOBT (8.11 g, 0.06 mol) were suspended in 120 ml of anhydrous DCM. After stirred in the room temperature for 20 min, L-phenylalanine methyl ester hydrochloride (11.86 g, 0.055 mol), EDC (11.50 g, 0.06 mol), and $Et_3N$ (12.63 g, 0.125 mol) were added successively. The resulting mixture was stirred for 24 h at room temperature. After the reaction complete monitored by TLC, the mixture was then concentrated and extracted with EtOAc (3 × 100 ml). Layers were separated and the organic layer was washed in turn with 1 M HCl (2 × 200 ml) and brine (2 × 200 ml), dried over anhydrous $Na_2SO_4$, filtered, and evaporated in vacuo to give compound **4** as white solid (13.7 g, 72.3%). Mp 209–210 °C, $^1$H NMR ($CDCl_3$-$d_6$, ppm): $\delta$ 2.58 (3H, s), 2.97 (1H, dd, $J$ = 6.9, 14.1 Hz), 3.12 (1H, dd, $J$ = 5.7, 14.1 Hz), 3.72(3H, s), 4.66 (1H, d, $J$ = 15.0 Hz), 4.83 (1H, m), 4.99 (1H, d, $J$ = 15.0 Hz), 6.74(1H, br), 6.83–7.84 (9H, m); ESI-MS *m/z*: 380.5 $[M+H]^+$.

### 5.2.5. (*R*)-2-(2-(3-Methyl-2-oxoquinoxalin-1(2*H*)-yl)acetamido)-3-phenylpropanoic (5)

Compound **4** (7.59 g, 0.02 mol) was mixed with a solution of 1 M KOH/EtOH (100 ml) and stirred in the room temperature for 6 h. The mixture was then concentrated in vacuo to provide the pale solid which was acidified to pH 4.0. The obtained precipitated

product was then collected and crystallized from EtOH to give compound **5** (6.23 g, 85.2%) as white solid. Mp 246–248 °C, ESI-MS: 366.3 $[M+H]^+$.

#### 5.2.6. (*R*)-2-(2-(3-Methyl-2-oxoquinoxalin-1(2*H*)-yl)acetamido)-3-phenylpropanoyl (6)

Compound **5** (0.73 g, 2 mmol) was dissolved in a mixed solution of $SOCl_2$ (40 ml) and DMF (1 ml), and stirred in the room temperature for 5 h. The resulting solution was rotary evaporated to get compound **6** as pale yellow crystal (0.68 g, 88.7%), which was used immediately in the next reaction without further purification.

#### 5.2.7. General procedures for the synthesis of compounds A1–A11

*o*-Toluidine (0.11 g, 1 mmol) was dissolved in anhydrous DCM (20 ml), *t*-BuOK (0.11 g, 1.02 mmol) was then added dropwise. After stirred at room temperature for approximately 20 min, compound **6** (0.38 g, 1 mmol) was added. The mixture was stirred for another 24 h at room temperature. After the reaction was completed monitoring by TLC, the mixture was then concentrated in vacuo and extracted with EtOAc (3 × 50 ml). Layers were separated and the organic layer was washed successively with 1 M HCl (2 × 50 ml) and brine (2 × 50 ml), dried over anhydrous $Na_2SO_4$, filtered, and the crude compounds A**1–A11** were purified by flash chromatography (PE:EA = 20:1–1:1) to provide the pure target products.

Compounds **A1**–**A11** were prepared following the procedures described above.

#### 5.2.8. (*S*)-2-(2-(3-Methyl-2-oxoquinoxalin-1(2*H*)-yl)acetamido)-*N*,3-diphenylpropanamide (A1)

Yellow solid, yield: 65.4%. mp 259–261 °C, $[\alpha]_D^{25} = +14.234$ (*c* 1, DMSO), ESI-MS 440.7 $[M+H]^+$, $^1H$ NMR (DMSO-$d_6$, ppm): $\delta$ 2.441 (s, 3H, $CH_3$), 2.883–2.921 (m, 1H, $CH_2$), 3.089–3.120 (m, 1H, $CH_2$), 4.699–4.737 (m, 1H, CHCO), 4.799 (d, *J* = 16.4 Hz, 1H, NCHCO), 5.006 (d, *J* = 16.2 Hz, 1H, NCHCO), 6.967 (d, *J* = 9 Hz, 1H, ArH), 7.068 (t, 1H, ArH), 7.244–7.331 (m, 8H, ArH), 7.405–7.430 (m, 1H, ArH), 7.582 (d, *J* = 7.8 Hz, 1H, ArH), 7.738 (dd, *J* = 1.2, 7.8 Hz, 1H, ArH), 8.876 (d, *J* = 8.4 Hz, 1H, CONH), 10.132 (s, 1H, CONH). Anal. Calcd for $C_{26}H_{24}N_4O_3$: C, 70.89; H, 5.49; N, 12.72. Found: C, 70.81; H, 5.42; N, 12.85.

#### 5.2.9. (*S*)-2-(2-(3-Methyl-2-oxoquinoxalin-1(2*H*)-yl)acetamido)-3-phenyl-*N*-(pyridine-3-yl) propanamide (A2)

Pale yellow solid, yield: 34.9%, mp 48–50 °C, $[\alpha]_D^{25} = +36.134$ (*c* 1, DMSO), ESI-MS 442.3 $[M+H]^+$, $^1H$ NMR (DMSO-$d_6$, ppm): $\delta$ 2.442 (s, 3H, $CH_3$), 2.904–2.943 (m, 1H, $CH_2$), 3.106–3.138 (m, 1H, $CH_2$), 4.707–4.745 (m, 1H, CHCO), 4.813 (d, *J* = 16.8 Hz, 1H, NCHCO), 5.017 (d, *J* = 16.2 Hz, 1H, NCHCO), 6.982 (d, *J* = 8.4 Hz, 1H, ArH), 7.233–7.436 (m, 9H, ArH), 7.739 (d, *J* = 7.8 Hz, 1H, ArH), 8.009 (d, *J* = 9 Hz, 1H, ArH), 8.284 (d, *J* = 4.8 Hz, 1H, ArH), 8.722 (s, 1H, ArH), 8.928 (d, *J* = 8.4 Hz, 1H, CONH), 10.357 (s, 1H, CONH). Anal. Calcd for $C_{25}H_{23}N_5O_3$: C, 68.01; H, 5.25; N, 15.86. Found: C, 67.89; H, 5.21; N, 15.97.

#### 5.2.10. (*S*)-2-(2-(3-Methyl-2-oxoquinoxalin-1(2*H*)-yl)acetamido)-3-phenyl-*N*-*p*-tolylpropan- amide (A3)

Yellow solid, yield: 46.9%, mp 277–278 °C, $[\alpha]_D^{25} = -11.579$ (*c* 1, DMSO), ESI-MS 455.3 $[M+H]^+$, $^1H$ NMR (DMSO-$d_6$, ppm): $\delta$ 2.25 (s, 3H, $CH_3$), 2.44 (s, 3H, $CH_3$), 2.89 (dd, *J* = 9.6, 13.2 Hz, 1H, $CH_2$), 3.09 (dd, *J* = 5.4, 13.8 Hz, 1H, $CH_2$), 4.75 (m, 2H, $NCH_2CO$), 5.01 (d, *J* = 16.2 Hz, 1H, CH), 6.96 (d, *J* = 8.4 Hz, 1H, ArH), 7.12–7.47 (m, 12H, ArH), 7.74 (d, *J* = 7.8 Hz, 1H, ArH), 8.86 (d, *J* = 7.8 Hz, 1H, ArH), 10.03 (s, 1H, CONH). Anal. Calcd for $C_{27}H_{26}N_4O_3$: C, 71.35; H, 5.77; N, 12.33. Found: C, 71.28; H, 5.68; N, 12.41.

#### 5.2.11. (*S*)-2-(2-(3-Methyl-2-oxoquinoxalin-1(2*H*)-yl)acetamido)-3-phenyl-*N*-*o*-tolylpropan-amide (A4)

Yellow solid, yield: 66.2%, mp 239–242 °C, $[\alpha]_D^{25} = +23.431$ (*c* 1, DMSO), ESI-MS 454.7 $[M+H]^+$, $^1H$ NMR (DMSO-$d_6$, ppm): $\delta$ 2.07 (s, 3H, $CH_3$), 2.45 (s, 3H, $CH_3$), 2.94 (dd, *J* = 9.6, 13.8 Hz, 1H, CH), 3.15 (dd, *J* = 5.4, 13.8 Hz, 1H, CH), 4.79 (m, 2H, $NCH_2CO$), 5.05 (d, *J* = 16.8 Hz, 1H, CHCO), 6.96 (d, *J* = 8.4 Hz, 1H, ArH), 7.08–7.42 (m, 11H, ArH), 7.74 (1H, d, *J* = 7.8 Hz, ArH), 8.88 (d, *J* = 8.4 Hz, 1H, ArH), 9.513 (s, 1H, CONH). Anal. Calcd for $C_{27}H_{26}N_4O_3$: C, 71.35; H, 5.77; N, 12.33. Found: C, 71.27; H, 5.69; N, 12.42.

#### 5.2.12. (*S*)-2-(2-(3-Methyl-2-oxoquinoxalin-1(2*H*)-yl)acetamido)-3-phenyl-*N*-*m*-tolylpropan- amide (A5)

Yellow solid, yield: 55.1%, mp 257–258 °C, $[\alpha]_D^{25} = +9.481$ (*c* 1, DMSO), ESI-MS 455.1 $[M+H]^+$, $^1H$ NMR (DMSO-$d_6$, ppm): $\delta$ 2.282 (3H, s, $CH_3$), 2.443 (s, 3H, $CH_3$), 2.891 (dd, *J* = 9.6, 13.2 Hz, 1H, CH), 3.098 (dd, *J* = 4.8, 13.8 Hz, 1H, CH), 4.682–4.720 (m, 1H, CH), 4.794 (d, *J* = 16.8 Hz, 1H, NCHCO), 4.011 (d, *J* = 16.8 Hz, 1H, NCHCO), 6.889 (d, *J* = 7.2 Hz, 1H, ArH), 6.968 (d, *J* = 8.4 Hz, 1H, ArH), 7.181–7.431 (m, 10H, ArH), 7.731–7.746 (m, 1H, ArH), 8.853 (d, *J* = 8.4 Hz, 1H, CONH), 10.034 (s, 1H, CONH). Anal. Calcd for $C_{27}H_{26}N_4O_3$: C, 71.35; H, 5.77; N, 12.33. Found: C, 71.24; H, 5.65; N, 12.41.

#### 5.2.13. (*S*)-*N*-(4-Fluorophenyl)-2-(3-methyl-2-oxoquinoxalin-1(2*H*)-yl)acetamido)-3-phenyl-propanamide (A6)

Yellow solid, yield: 55.2%, mp 248–250 °C, $[\alpha]_D^{25} = +32.325$ (*c* 1, DMSO), ESI-MS 459.3 $[M+H]^+$, $^1H$ NMR (DMSO-$d_6$, ppm): $\delta$ 2.441 (s, 3H, $CH_3$), 2.878–2.911 (m, 1H, $CH_2$), 3.058–3.009 (m, 1H, $CH_2$), 4.693 (m, 1H, CH), 4.805 (d, *J* = 16.8 Hz, 1H, NCHCO), 5.002 (d, *J* = 16.8 Hz, 1H, NCHCO), 6.970 (d, *J* = 8.4 Hz, 1H, ArH), 7.241–7.554 (m, 11H, ArH), 7.726 (d, *J* = 8.4 Hz, 1H, ArH), 8.798 (d, *J* = 7.8 Hz, 1H, CONH), 10.269 (s, 1H, CONH). Anal. Calcd for $C_{26}H_{23}FN_4O_3$: C, 68.11; H, 5.06; N, 12.22. Found: C, 68.04; H, 4.97; N, 12.31.

#### 5.2.14. (*S*)-*N*-(4-Chlorophenyl)-2-(3-methyl-2-oxoquinoxalin-1(2*H*)-yl)acetamido)-3-phenyl- propanamide (A7)

Red powder, yield: 39.8%, mp 285–287 °C, $[\alpha]_D^{25} = -15.268$ (*c* 1, DMSO), ESI-MS 475.8 $[M+H]^+$, $^1H$ NMR (DMSO-$d_6$, ppm): $\delta$ 2.440 (s, 3H, $CH_3$), 2.902 (dd, *J* = 9.6, 13.2 Hz, 1H, $CH_2$), 3.095 (dd, *J* = 5.4, 13.8 Hz, 1H, $CH_2$), 4.675–4.714 (m, 1H, CH), 4.802 (d, *J* = 16.8 Hz, 1H, $NCH_2CO$), 5.005 (d, *J* = 16.8 Hz, 1H, $NCH_2CO$), 6.971 (d, *J* = 8.4 Hz, 1H, ArH), 7.239–7.436 (m, 9H, ArH), 7.596–7.616 (m, 2H, ArH), 7.737 (dd, *J* = 1.2, 7.8 Hz, 1H, ArH), 8.899 (d, *J* = 8.4 Hz, 1H, CONH), 10.270 (s, 1H, CONH). Anal. Calcd for $C_{26}H_{23}ClN_4O_3$: C, 65.75; H, 4.88; N, 11.80. Found: C, 65.66; H, 4.74; N, 11.93.

#### 5.2.15. (*S*)-*N*-(4-Bromophenyl)-2-(3-methyl-2-oxoquinoxalin-1(2*H*)-yl)acetamido)-3-phenyl- propanamide (A8)

Yellow solid, yield: 64.2%, mp 269–271 °C, $[\alpha]_D^{25} = +20.123$ (*c* 1, DMSO), ESI-MS 520.4 $[M+H]^+$, $^1H$ NMR (DMSO-$d_6$, ppm): $\delta$ 2.40 (s, 3H, $CH_3$), 2.882–2.921 (m, 1H, $CH_2$), 3.078–3.109 (m, 1H, $CH_2$), 4.693 (m, 1H, CH), 4.803 (d, *J* = 16.8 Hz, 1H, NCHCO), 5.004 (d, *J* = 16.8 Hz, 1H, NCHCO), 6.973 (d, *J* = 8.4 Hz, 1H, ArH), 7.249–7.564 (m, 11H, ArH), 7.737 (d, *J* = 8.4 Hz, 1H, ArH), 8.898 (d, *J* = 7.8 Hz, 1H, CONH), 10.267 (s, 1H, CONH). Anal. Calcd for $C_{26}H_{23}BrN_4O_3$: C, 60.12; H, 4.46; N, 10.79. Found: C, 59.95; H, 4.41; N, 10.87.

#### 5.2.16. (*S*)-*N*-(3,4-Difluorophenyl)-2-(3-methyl-2-oxoquinoxalin-1(2*H*)-yl)acetamido)-3- phenylpropanamide (A9)

Yellow solid, yield: 44.3%, mp 271–273 °C, $[\alpha]_D^{25} = -24.413$ (*c* 1, DMSO), ESI-MS 476.7 $[M+H]^+$, $^1H$ NMR (DMSO-$d_6$, ppm): $\delta$

2.441 (s, 3H, $CH_3$), 2.886–2.925 (m, 1H, $CH_2$), 3.088–3.104 (m, 1H, $CH_2$), 4.663 (s, 1H, CH), 4.805 (d, $J$ = 17.4 Hz, 1H, NCHCO), 5.006 (d, $J$ = 16.2 Hz, 1H, NCHCO), 6.976 (d, $J$ = 9 Hz, 1H, ArH), 7.253–7.422 (m, 9H, ArH), 7.732–7.743 (m, 2H, ArH), 8.924 (d, $J$ = 7.8 Hz, 1H, CONH), 10.381 (s, 1H, CONH). Anal. Calcd for $C_{26}H_{22}F_2N_4O_3$: C, 65.54; H, 4.65; N, 11.76. Found: C, 65.48; H, 4.56; N, 11.83.

#### 5.2.17. (*S*)-*N*-(3,4-Dichlorophenyl)-2-(3-methyl-2-oxoquinoxalin-1(2*H*)-yl)acetamido)-3- phenylpropanamide (A10)

Yellow solid, yield: 44.5%, mp 251–253 °C, $[\alpha]_D^{25} = -16.09$ ($c$ 1, DMSO), ESI-MS 510.1 $[M+H]^+$, $^1$H NMR (DMSO-$d_6$, ppm): $\delta$ 2.443 (s, 3H, $CH_3$), 2.911 (dd, $J$ = 9.6, 13.8 Hz, 1H, CH), 3.1 (dd, $J$ = 5.4, 13.8 Hz, 1H, CH), 4.669 (d, $J$ = 4.2 Hz, 1H, CH), 4.815 (d, $J$ = 16.2 Hz, 1H, $NCH_2CO$), 5.004 (d, $J$ = 16.8 Hz, 1H, NCHCO), 6.993 (d, $J$ = 8.4 Hz, 1H, ArH), 7.252–7.333 (m, 6H, ArH), 7.427 (t, $J$ = 8.4 Hz, 1H, ArH), 7.487 (dd, $J$ = 1.8, 8.4 Hz, 1H, ArH), 7.583 (d, $J$ = 9 Hz, 1H, ArH), 7.74 (dd, $J$ = 1.8, 8.4 Hz, 1H, ArH), 7.956 (d, $J$ = 2.4 Hz, 1H, ArH), 8.923 (d, $J$ = 8.4 Hz, 1H, CONH), 10.406 (s, 1H, CONH). Anal. Calcd for $C_{26}H_{22}Cl_2N_4O_3$: C, 61.31; H, 4.35; N, 11.00. Found: C, 61.28; H, 4.26; N, 11.17.

#### 5.2.18. (*S*)-*N*-(3-Chloro-4-fluorophenyl)-2-(3-methyl-2-oxoquinoxalin-1(2*H*)-yl)acetamido)-3- phenylpropanamide (A11)

White solid, mp 251–253 °C, $[\alpha]_D^{25} = +13.481$ ($c$ 1, DMSO), ESI-MS 493.9 $[M+H]^+$, $^1$H NMR (DMSO-$d_6$, ppm): $\delta$ 2.45 (s, 3H, $CH_3$), 2.91 (dd, $J$ = 9.6, 13.2 Hz, 1H, $CH_2$), 3.10 (dd, $J$ = 5.4, 13.8 Hz, 1H, $CH_2$), 4.66 (m, 2H, $NCH_2CO$), 5.00 (d, $J$ = 16.8 Hz, 1H, CH), 6.99 (d, $J$ = 8.4 Hz, 1H, ArH), 7.24–7.47 (m, 9H, ArH), 7.74 (d, $J$ = 7.8 Hz, 1H, ArH), 7.88 (dd, $J$ = 2.4, 6.6 Hz, 1H, ArH), 8.92 (d, $J$ = 7.8 Hz, 1H, ArH), 10.33 (s, 1H, CONH). Anal. Calcd for $C_{26}H_{22}ClFN_4O_3$: C, 63.35; H, 4.50; N, 11.37. Found: C, 63.28; H, 4.41; N, 12.45.

#### 5.2.19. General procedures for the synthesis of compounds A12–A19

Compound **A16** (0.3 g, 0.82 mmol), HOBT (0.13 g, 0.99 mmol) were suspended in anhydrous DCM (40 ml) and after stirred in the room temperature for 20 min, diethylamine (0.07 g, 0.99 mmol), EDC (0.19 g, 0.99 mmol), and $Et_3N$ (0.166 g, 1.62 mmol) were added. And the mixture was stirred for 24 h at room temperature. After the reaction complete, the mixture was then concentrated and extracted with EtOAc (3 × 50 ml).Layers were separated and the organic layer was washed with 1 M HCl (2 × 50 ml) and brine (2 × 50 ml), dried over $Na_2SO_4$, filtered, and the pure target products **A16** were obtained by flash chromatography (PE:EA = 10:1–1:1).

Compounds of **A12–A19** were synthesized following the general procedure as described above.

#### 5.2.20. (*S*)-2-(2-(3-Methyl-2-oxoquinoxalin-1(2*H*)-yl)acetamido)-3-phenyl-*N*-propylpropan- amide (A12)

White solid, yield: 48.7%, mp 283.5–285 °C, $[\alpha]_D^{25} = +24.019$ ($c$ 1, DMSO), ESI-MS 407.4 $[M+H]^+$, $^1$H NMR (DMSO-$d_6$, ppm): $\delta$ 0.790 (t, $J$ = 7.2 Hz, 3H, $CH_3$), 1.355–1.391 (m, 2H, $CH_2$), 2.438 (s, 3H, $CH_3$), 2.785 (dd, $J$ = 9.6,13.8 Hz, 1H, CH), 2.969–3.059 (m, 3H, $CH_2$, CH), 4.469–4.507 (m, 1H, CH), 4.721 (d, $J$ = 16.8 Hz, 1H, NCHCO), 5.023 (d, $J$ = 16.8 Hz, 1H, NCHCO), 6.904 (d, $J$ = 8.4 Hz, 1H, ArH), 7.230–7.327 (m, 6H, ArH), 7.732–7.410 (m, 1H, ArH), 7.724–7.740 (m, 1H, ArH), 8.022 (t, $J$ = 6 Hz, 1H, CONH), 8.693 (d, $J$ = 9 Hz, 1H, CONH). Anal. Calcd for $C_{23}H_{26}N_4O_3$: C, 67.96; H, 6.45; N, 13.78. Found: C, 67.89; H, 6.38; N, 13.85.

#### 5.2.21. (*S*)-*N*-Butyl-2-(2-(3-methyl-2-oxoquinoxalin-1(2*H*)-yl)acetamido)-3-phenylpropan-amide (A13)

White solid, yield: 58.9%, mp 267–269 °C, $[\alpha]_D^{25} = +26.481$ ($c$ 1, DMSO), ESI-MS 420.8 $[M+H]^+$, $^1$H NMR (DMSO-$d_6$, ppm): $\delta$ 0.843 (t, $J$ = 7.2 Hz, 3H, $CH_3$), 1.179–1.241 (m, 2H, $CH_2$), 1.313–1.362 (m, 2H, $CH_2$), 2.440 (s, 3H, $CH_3$), 2.764–3.095 (m, 4H, $CH_2$), 4.465–4.503 (m, 1H, CH), 4.725 (d, $J$ = 16.8 Hz, 1H, NCHCO), 5.02 (d, $J$ = 16.8 Hz, 1H, NCHCO), 6.912 (d, $J$ = 7.8 Hz, 1H, ArH), 7.237–7.327 (m, 6H, ArH), 7.397 (t, $J$ = 8.4 Hz, 1H, ArH), 7.733 (d, $J$ = 7.8 Hz, 1H, ArH), 8.000 (t, $J$ = 5.4 Hz, 1H, CONH), 8.695 (d, $J$ = 9 Hz, 1H, CONH). Anal. Calcd for $C_{24}H_{28}N_4O_3$: C, 68.55; H, 6.71; N, 13.32. Found: C, 68.48; H, 6.68; N, 13.47.

#### 5.2.22. (*S*)-*N*,*N*-Diethyl-2-(2-(3-methyl-2-oxoquinoxalin-1(2*H*)-yl)acetamido)-3-phenyl- propanamide (A14)

White solid, yield: 68.1%, mp 176–178 °C, $[\alpha]_D^{25} = +19.481$ ($c$ 1, DMSO), ESI-MS 421.3 $[M+H]^+$, $^1$H NMR (DMSO-$d_6$, ppm): $\delta$ 0.933–0.975 (m, 6H, $CH_3$), 2.438 (s, 3H, $CH_3$), 2.835 (dd, $J$ = 8.4, 13.8 Hz, 1H, CH), 2.966 (dd, $J$ = 6.6, 13.2 Hz, 1H, CH), 3.097–3.379 (m, 4H, $NCH_2$,), 4.735 (d, $J$ = 16.8 Hz, 1H, NCHCO), 4.811–4.850 (m, 1H, CH), 4.996 (d, $J$ = 17.4 Hz, 1H, NCHCO), 6.888 (d, $J$ = 7.8 Hz, 1H, ArH), 7.245–7.328 (m, 6H, ArH), 7.403–7.429 (m, 1H, ArH), 7.727–7.742 (m, 1H, ArH), 8.934 (d, $J$ = 9 Hz, 1H, CONH). Anal. Calcd for $C_{24}H_{28}N_4O_3$: C, 68.55; H, 6.71; N, 13.32. Found: C, 68.64; H, 6.64; N, 13.21.

#### 5.2.23. (*S*)-*N*-Isopropyl-2-(2-(3-methyl-2-oxoquinoxalin-1(2*H*)-yl)acetamido)-3-phenyl- propanamide (A15)

White solid, yield: 55.1%, mp 285–287 °C, $[\alpha]_D^{25} = +17.270$ ($c$ 1, DMSO), ESI-MS 406.8 $[M+H]^+$, $^1$H NMR (DMSO-$d_6$, ppm): $\delta$ 0.973 (d, $J$ = 6.6 Hz, 3H, $CH_3$), 1.045 (d, $J$ = 6.6 Hz, 3H, $CH_3$), 2.441 (s, 3H, $CH_3$), 2.782 (dd, $J$ = 9.6, 13.8 Hz, 1H, CH), 2.965 (dd, $J$ = 5.4, 13.2 Hz, 1H, CH), 3.788–3.845 (m, 1H, CH), 4.452–4.490 (m, 1H, CH), 4.74 (d, $J$ = 16.8 Hz, 1H, NCHCO), 4.991 (d, $J$ = 16.8 Hz, 1H, NCHCO), 6.949 (d, $J$ = 7.8 Hz, 1H, ArH), 7.228–7.431 (m, 7H, ArH), 7.738 (dd, $J$ = 1.2, 7.8 Hz, 1H, ArH), 7.860 (d, $J$ = 7.8 Hz, 1H, CONH), 8.646 (d, $J$ = 9 Hz, 1H, CONH). Anal. Calcd for $C_{23}H_{26}N_4O_3$: C, 67.96; H, 6.45; N, 13.78. Found: C, 67.87; H, 6.38; N, 13.84.

#### 5.2.24. (*R*)-Methyl4-methyl-2-((*S*)-2-(2-(3-methyl-2-oxoquinoxalin-1(2*H*)-yl)acetamido)- 3-phenylpropanamide (A16)

White solid, yield: 35.6%, mp 241–242 °C, $[\alpha]_D^{25} = +32.92$ ($c$ 1, DMSO), ESI-MS 492.6 $[M+H]^+$, $^1$H-NMR (DMSO-$d_6$, ppm): $\delta$ 0.8335 (d, $J$ = 6.6 Hz, 3H, $CH_3$), 0.882 (d, $J$ = 6 Hz, 3H, $CH_3$), 1.504–1.608 (m, 3H, CH, $CH_2$), 2.435 (s, 3H, $CH_3$), 2.762 (dd, $J$ = 10.8, 13.8 Hz, 2H, $CH_2$), 3.064 (dd, $J$ = 4.2, 14.4 Hz, 1H, NCH), 3.628 (s, 3H, $CH_3$), 4.299–4.337 (m, 1H, CHCO), 4.587–4.625 (m, 1H, CHCO), 4.695 (d, $J$ = 16.8 Hz, 1H, NCHCO), 4.984 (d, $J$ = 16.8 Hz, 1H, NCHCO), 6.829 (d, $J$ = 8.4 Hz, 1H, ArH), 7.247–7.325 (m, 6H, ArH), 7.379 (t, $J$ = 7.2 Hz, 1H, ArH), 7.730 (d, $J$ = 7.8 Hz, 1H, ArH), 8.489 (d, $J$ = 7.8 Hz, 1H, CONH), 8.712 (d, $J$ = 9 Hz, 1H, CONH). Anal. Calcd for $C_{27}H_{32}N_4O_5$: C, 65.84; H, 6.55; N, 13.37. Found: C, 65.78; H, 6.41; N, 13.43.

#### 5.2.25. (*S*)-Methyl 4-(2-(2-(3-methyl-2-oxoquinoxalin-1(2*H*)-yl)acetamido)-3-phenylpropan- amido)butanoate (A17)

Yellow solid, yield: 64.5%, mp 213–215 °C, $[\alpha]_D^{25} = -21.27$ ($c$ 1, DMSO), ESI-MS 465.1 $[M+H]^+$, $^1$H NMR (DMSO-$d_6$, ppm): $\delta$ 1.194 (t, $J$ = 14.4 Hz, 2H, $CH_2$), 1.612–1.624 (m, 2H, $CH_2$), 2.224–2.250 (m, 2H, $CH_2N$), 2.439 (s, 3H, $CH_3$), 2.775–2.813 (m, 1H, $CH_2$), 3.295–3.047 (m, 1H, $CH_2$), 3.585 (s, 1H, $CH_3O$), 4.458–4.466 (m, 1H, CH), 4.745 (d, $J$ = 16.8 Hz, 1H, NCHCO), 5.026 (d, $J$ = 16.8 Hz, 1H, NCHCO), 6.936 (d, $J$ = 8.4 Hz, 1H, ArH), 7.225–7.327 (m, 6H, ArH), 7.401 (t, $J$ = 8.4 Hz, 1H, ArH), 7.734 (d, $J$ = 7.8 Hz, 1H, ArH), 8.104 (t, $J$ = 5.4 Hz, 1H, CONH), 8.745 (d, $J$ = 8.4 Hz, 1H, CONH). Anal. Calcd for $C_{25}H_{28}N_4O_5$: C, 64.64; H, 6.08; N, 12.06. Found: C, 64.52; H, 5.98; N, 12.14.

#### 5.2.26. (*S*)-Methyl 6-(2-(2-(3-methyl-2-oxoquinoxalin-1(2*H*)-yl)acetamido)-3-phenylpropan- amido)hexanoate (A18)

Yellow solid, yield: 67.1%, mp 236–239 °C, $[\alpha]_D^{25} = -22.121$ (*c* 1, DMSO), ESI-MS 493.4 $[M+H]^+$, $^1H$ NMR (DMSO-$d_6$, ppm): $\delta$ 1.161–1.211 (m, 2H, $CH_2$), 1.319–1.367 (m, 2H, $CH_2$), 1.465–1.515 (m, 2H, $CH_2$), 2.262 (t, $J$ = 7.8 Hz, 2H, $CH_2CO$), 2.438 (s, 3H, $CH_3$), 2.762–2.800 (m, 1H, $CH_2$), 2.981–3.022 (m, 2H, $CH_2N$), 3.040–3.083 (m, 1H, $CH_2$), 3.576 (s, 1H, $CH_3O$), 4.457–4.496 (m, 1H, CH), 4.725 (d, $J$ = 16.8 Hz, 1H, NCHCO), 5.018 (d, $J$ = 16.8 Hz, 1H, NCHCO), 6.912 (d, $J$ = 8.4 Hz, 1H, ArH), 7.234–7.324 (m, 6H, ArH), 7.385–7.413 (m, 1H, ArH), 7.732 (dd, $J$ = 1.2, 7.8 Hz, 1H, ArH), 8.104 (t, $J$ = 5.4 Hz, 1H, CONH), 8.691 (d, $J$ = 9 Hz, 1H, CONH). Anal. Calcd for $C_{27}H_{32}N_4O_5$: C, 65.84; H, 6.55; N, 11.37. Found: C, 65.72; H, 6.48; N, 11.41.

#### 5.2.27. Methyl 4-((*S*)-2-(2-(3-methyl-2-oxoquinoxalin-1(2*H*)-yl)acetamido)-3-phenylpropan- amido)-4-(methylthio)butanoate (A19)

Red solid, yield: 51.1%, mp 208–210 °C, $[\alpha]_D^{25} = +23.900$ (*c* 1, DMSO), ESI-MS 510.9 $[M+H]^+$, $^1H$ NMR (DMSO-$d_6$, ppm): $\delta$ 1.827–2.039 (m, 5H, $CH_3S$, $CH_2$), 2.282–2.436 (m, 5H, $CH_3$, $CH_2$), 2.760–2.816 (m, 1H, CH), 2.983–3.073 (m, 1H, CH), 3.639 (s, 3H, $CH_3O$), 4.379–4.438 (m, 1H, CH), 4.580–4.652 (m, 1H, CH), 4.703–4.758 (m, 1H, NCHCO), 4.946–5.019 (m, 1H, NCHCO), 6.82 (d, $J$ = 8.4 Hz, 1H, ArH), 7.223–7.332 (m, 7H, ArH), 7.406 (dd, $J$ = 8.4, 16.8 Hz, 1H, ArH), 7.725 (s, 1H, ArH), 8.531 (d, $J$ = 9.6 Hz, 1H, CONH), 8.707 (d, $J$ = 8.4 Hz, 1H, CONH). Anal. Calcd for $C_{26}H_0N_4O_5S$: C, 61.16; H, 5.92; N, 10.97. Found: C, 61.02; H, 5.85; N, 11.03.

### 5.3. Enzymatic inhibition assay (in vitro)

#### 5.3.1. MMP-2 inhibition assay

Gelatinase A (MMP-2) assay was performed as described by Baragi et al.[30] The gelatinase, substrate (succinylated gelatin) and inhibitor were dissolved in sodium borate buffer (pH 8.5, 50 mM) and incubated for 30 min at 37 °C, and then 0.03% trinitrobenzenesulfonic acid (TNBS, Sigma) was added and incubated for another 20 min, the resulting solution was detected under 450 nm wavelength to gain absorption.

#### 5.3.2. APN inhibition assay

The $IC_{50}$ values against APN were determined by using L-Leu-*p*-nitroanilide as substrate and microsomal aminopeptidase from Porcine Kidney Mocrosomes (Sigma) as the enzyme in 50 mM PBS, pH 7.2 at 37 °C.[31] The hydrolysis of the substrate was monitored by following the change in the absorbance measured at 405 nm with a UV–vis spectrophotometer, Pharmacia LKB, Biochrom 4060. All the solutions of inhibitors were prepared in the assay buffer, and the pH was adjusted to 7.5 by the addition of 0.1 M HCl or 0.1 M NaOH. All the inhibitors were preincubated with APN for 30 min at room temperature. The assay mixture, which contained the inhibitor solution (concentration dependent on the inhibitor), the enzyme solution (4 μg/ml final concentration), and the assay buffer, was adjusted to 200 μl.

### 5.4. MTT assay

The cell lines were grown in RPMI1640 medium containing 10% FBS at 37 °C in a humidified incubator with 5% $CO_2$. Cell proliferation was determined by the MTT (3-[4,5-dimethyl-2-thiazolyl]-2,5-diphenyl-2*H*-tetrazolium bromide) assay. Briefly, cells were plated in a 96-well plate at 10,000 cells per well, cultured for 4 h in complete growth medium, then treated with 1600, 800, 400, 200, or 100 μg/ml of the compounds for 48 h. Following this, 0.5% MTT solution was added to each well. After further incubation for 4 h, the formazan formed from MTT was extracted by adding DMSO and mixing for 15 min. The optical density was read with ELISA reader at 570 nm.

### 5.5. Computational-docking assay

The docking study was performed as follows: The selected compound was constructed with a Sybyl/Sketch module and optimized using Powell Energetic Gradiet method with a Tripos force field with the convergence criterion set at 0.05 kcal/mol Å, and assigned with Gasteiger-Hückel method.[32,33] When it comes to the docking assay of MMP-2, residues in a radius of 4.0 Å around SC-74020 (the provided ligand of MMP-2 in the crystal structure. PDB code: 1HOV)[29] were selected as the active site, including the zinc(II) ion. As to APN, the residues in a radius of 7.0 Å around bestatin (the provided ligand of APN in the co-crystal structure, PDB code: 2DQM)[34] were selected as the active site, and other docking parameters implied in the program were kept default.

## Acknowledgements

This work was financial supported from the Natural Science Foundation of China (30701053), the doctoral Foundation of Ministry of Education of the People's Republic of China (20070422061), and the Natural Science Foundation of Shandong Province (Y2008C01).

## References and notes

1. Kohrmann, A.; Kammerer, U.; Kapp, M.; Dietl, J.; Anacker, J. *BMC Cancer* **2009**, *9*, 188.
2. Coussens, L. M.; Fingleton, B.; Matrisian, L. M. *Science* **2002**, *295*, 2387.
3. Pavlaki, M.; Zucker, S. *Cancer Metastasis Rev.* **2003**, *22*, 177.
4. Michaelides, M. R.; Curtin, M. L. *Curr. Pharm. Des.* **1999**, *5*, 787.
5. Nishida, Y.; Miyamori, H.; Thompson, E. W.; Takino, T.; Endo, Y.; Sato, H. *Cancer Res.* **2008**, *68*, 9096.
6. Bjorklund, M.; Koivunen, E. *Biochim. Biophys. Acta* **2005**, *1755*, 37.
7. Lovejoy, B.; Welch, A. R.; Carr, S.; Luong, C.; Broka, C.; Hendricks, R. T.; Campbell, J. A.; Walker, K. A.; Martin, R.; Van Wart, H.; Browner, M. F. *Nat. Struct. Biol.* **1999**, *6*, 217.
8. Verma, R. P.; Hansch, C. *Bioorg. Med. Chem.* **2007**, *15*, 2223.
9. Becker, J. W.; Marcy, A. I.; Rokosz, L. L.; Axel, M. G.; Burbaum, J. J.; Fitzgerald, P. M. D.; Cameron, P. M.; Esser, C. K.; Hagmann, W. K.; Hermes, J. D.; Springer, J. P. *Protein Sci.* **1995**, *4*, 1966.
10. Kontogiorgis, C. A.; Papaioannou, P.; Hadjipavlou-Litina, D. J. *Curr. Med. Chem.* **2005**, *12*, 339.
11. Cheng, X. C.; Wang, Q.; Fang, H.; Tang, W.; Xu, W. F. *Bioorg. Med. Chem.* **2008**, *16*, 7932.
12. Cheng, X. C.; Wang, Q.; Fang, H.; Tang, W.; Xu, W. F. *Bioorg. Med. Chem.* **2008**, *16*, 5398.
13. Cheng, X. C.; Wang, Q.; Fang, H.; Tang, W.; Xu, W. F. *Eur. J. Med. Chem.* **2008**, *43*, 2130.
14. Li, X.; Li, Y.; Xu, W. *Bioorg. Med. Chem.* **2006**, *14*, 1287.
15. Zhang, L.; Zhang, J.; Fang, H.; Wang, Q.; Xu, W. *Bioorg. Med. Chem.* **2006**, *14*, 8286.
16. Li, Y. L.; Xu, W. F. *Bioorg. Med. Chem.* **2004**, *12*, 5171.
17. Qu, X. J.; Yuan, Y. X.; Tian, Z. G.; Xu, W. F.; Chen, M. H.; Cui, S. X.; Guo, Q.; Gai, R.; Makuuchi, M.; Nakata, M.; Tang, W. *Int. J. Mol. Med.* **2006**, *18*, 609.
18. Qu, X.; Yuan, Y.; Xu, W.; Chen, M.; Cui, S.; Meng, H.; Li, Y.; Makuuchi, M.; Nakata, M.; Tang, W. *Anticancer Res.* **2006**, *26*, 3573.
19. Li, X.; Yang, K. H.; Li, W. L.; Xu, W. F. *Drug Future* **2006**, *31*, 979.
20. Nemoto, H.; Cai, J.; Asao, N.; Iwamoto, S.; Yamamoto, Y. *J. Med. Chem.* **1995**, *38*, 1673.
21. Otani, T. T.; Briley, M. R. *J. Pharm. Sci.* **1985**, *74*, 40.
22. Li, X.; Wang, D. H.; Wu, J. F.; Xu, W. F. *Synth. Commun.* **2005**, *35*, 1.
23. Terauchi, M.; Kajiyama, H.; Shibata, K.; Ino, K.; Nawa, A.; Mizutani, S.; Kikkawa, F. *BMC Cancer* **2007**, *7*, 140.
24. Pasqualini, R.; Koivunen, E.; Kain, R.; Lahdenranta, J.; Sakamoto, M.; Stryhn, A.; Ashmun, R. A.; Shapiro, L. H.; Arap, W.; Ruoslahti, E. *Cancer Res.* **2000**, *60*, 722.
25. Gabrilovac, J.; Breljak, D.; Čupić, B. *Int. Immunopharmacol.* **2008**, *8*, 613.
26. Mishima, Y.; Matsumoto-Mishima, Y.; Terui, Y.; Katsuyama, M.; Yamada, M.; Mori, M.; Ishizaka, Y.; Ikeda, K.; Watanabe, J.; Mizunuma, N.; Hayasawa, H.; Hatake, K. *J. Natl. Cancer Inst.* **2002**, *94*, 1020.
27. Yuan, Y. X.; Xu, W. F.; Liu, J.; Chen, M. H.; Meng, H.; Qu, X. J. *Ai zheng* **2006**, *25*, 663.
28. SYBYL6.91. Tripos Associates. 1699 S. Hanley Road, Suite 303. St. Louis, MO 63144–2913, 2003.

29. Feng, Y.; Likos, J. J.; Zhu, L.; Woodward, H.; Munie, G.; McDonald, J. J.; Stevens, A. M.; Howard, C. P.; De Crescenzo, G. A.; Welsch, D.; Shieh, H. S.; Stallings, W. C. *Biochim. Biophys. Acta* **2002**, *1598*, 10.
30. Baragi, V. M.; Shaw, B. J.; Renkiewicz, R. R.; Kuipers, P. J.; Welgus, H. G.; Mathrubutham, M.; Cohen, J. R.; Rao, S. K. *Matrix Biol.* **2000**, *19*, 267.
31. Lejczak, B.; Kafarski, P.; Zygmunt, J. *Biochemistry* **1989**, *28*, 3549.
32. GALAHADTM is distributed by Tripos Inc., 1699 South Hanley Rd., St. Louis, Missouri, USA (http://www.tripos.com).
33. Richmond, N. J.; Abrams, C. A.; Wolohan, P. R.; Abrahamian, E.; Willett, P.; Clark, R. D. *J. Comput. Aided Mol. Des.* **2006**, *20*, 567.
34. Berman, H. M.; Westbrook, J.; Feng, Z.; Gilliland, G.; Bhat, T. N.; Weissig, H.; Shindyalov, I. N.; Bourne, P. E. *Nucleic Acids Res.* **2000**, *28*, 235.